Letter Vol. 2, No. 10 / October 2015 / Optica 850

optica

Cloaked contact grids on solar cells by coordinate transformations: designs and prototypes

MARTIN F. SCHUMANN, 1,2,* SAMUEL WIESENDANGER, JAN CHRISTOPH GOLDSCHMIDT, BENEDIKT BLÄSI, KARSTEN BITTKAU, ULRICH W. PAETZOLD, ALEXANDER SPRAFKE, RALF B. WEHRSPOHN, CARSTEN ROCKSTUHL, 2,8 AND MARTIN WEGENER, ALEXANDER SPRAFKE, ALEXANDER SPRAFKE, RALF B. WEHRSPOHN, ALEXANDER SPRAFKE, ALEXANDER SPRA

¹Institute of Applied Physics, Karlsruhe Institute of Technology (KIT), 76128 Karlsruhe, Germany

²Institute of Nanotechnology, Karlsruhe Institute of Technology (KIT), 76021 Karlsruhe, Germany

³Institute of Condensed Matter Theory and Solid State Optics, Friedrich-Schiller-Universität Jena, 07743 Jena, Germany

⁴Fraunhofer Institute for Solar Energy Systems ISE, Heidenhofstraße 2, 79110 Freiburg, Germany

⁵Institut für Energie und Klimaforschung (IEK-5), Forschungszentrum Jülich GmbH, 52425 Jülich, Germany

⁶Institute of Physics, Martin-Luther-University Halle-Wittenberg, 06120 Halle, Germany

⁷Fraunhofer Institute for Microstructure of Materials and Systems IMWS, 06120 Halle, Germany

⁸Institute of Theoretical Solid-State Physics, Karlsruhe Institute of Technology (KIT), 76128 Karlsruhe, Germany

*Corresponding author: martin.schumann@kit.edu

Received 29 April 2015; revised 28 August 2015; accepted 28 August 2015 (Doc. ID 239917); published 25 September 2015

Nontransparent contact fingers on the sun-facing side of solar cells represent optically dead regions which reduce the energy conversion per area. We consider two approaches for guiding the incident light around the contacts onto the active area. The first approach uses graded-index metamaterials designed by two-dimensional Schwarz-Christoffel conformal maps, and the second uses freeform surfaces designed by one-dimensional coordinate transformations of a point to an interval. We provide proof-of-principle demonstrators using direct laser writing of polymer structures on silicon wafers with opaque contacts. Freeform surfaces are amenable to mass fabrication and allow for complete recovery of the shadowing effect for all relevant incidence angles. © 2015 Optical Society of America

OCIS codes: (160.3918) Metamaterials; (350.3950) Micro-optics; (230.4000) Microstructure fabrication; (350.6050) Solar energy.

http://dx.doi.org/10.1364/OPTICA.2.000850

Today, when extracting electrical power from photovoltaic (PV) devices, every improvement matters. To reduce serial Ohmic resistance losses otherwise limiting the PV efficiency, metallic fingers and bus bar grids on the sun-facing surface of crystalline silicon solar cells are required. Likewise, interconnecting bus bar lines between cell stripes in thin-film PV modules are also necessary. All of these contact schemes create significant shading losses of the PV modules such that the overall active area is reduced by a few percent, resulting in correspondingly decreased power-conversion efficiencies [1]. If a contact could be made "invisible" by guiding the incident light around it and absorbing the light within the PV active region, this loss would be recovered. One might then even consider increasing the fractional metal contact area on top of the PV cell to further reduce the serial Ohmic resistance.

The contact shadowing problem has been recognized previously: proposed concepts like refracting triangular grooves in a dielectric layer on top of the PV cell [2,3] or experimentally realized reflecting triangular metal contacts called light-harvesting strings [4] have already provided partial remedy. However, can the shadow effect be eliminated completely? What are the practical limits?

Recently, ideal invisibility cloaks have been designed theoretically by mapping coordinate transformations, which exclude a certain region from space, onto spatially inhomogeneous and anisotropic material distributions. Theoretically, these devices could be integrated into the solar cell where they serve the purpose of perfectly molding the flow of light around the metal contact and onto the PV cell active area for any angle of incidence and any polarization of light. Intuitively, one can think of the resulting structures as anisotropic yet polarization-independent gradedindex lenses. However, the required electric permittivity $\stackrel{\leftrightarrow}{arepsilon}$ and magnetic permeability \overrightarrow{u} tensors within these ideal cloaks contain elements with zeros and infinities [5]. For the broad spectral range relevant for solar energy conversion, however, nature has only provided us with transparent dielectrics with refractive indices n within the rather limited range of about n = 1 - 3 $(\Leftrightarrow \varepsilon = 1 - 9 \text{ and } \mu = 1)$. Hence, such ideal cloaks are far from being practical. There is, however, room for simplifications: first, a large fraction of the sunlight impinges onto the PV cell with near normal incidence. Angles beyond few tens of degrees with respect to the surface normal are of lesser importance. This means that an ideal omnidirectional cloak is not needed. Second, ideal cloaks also preserve the light phase. This aspect is not relevant for the purpose of solar energy conversion either.

In this Letter, by using coordinate transformations, we design devices that offer a trade-off between invisible-contact performance and practical accessibility. Since typical solar cell contacting schemes feature metal fingers with lengths at least an order of magnitude larger than their widths, we consider the fingers to be infinitely elongated along the z axis and parallel to the PV cell plane, such that the problem can effectively be treated within the xy plane. We choose the y axis to be normal to the PV cell surface at y=0. Pendry's famous coordinate transformation [5] of a (by definition invisible) point to a cloaked circle of radius R_1 is illustrated in Fig. 1(a). It is restricted to a radius of $R_2 \ge R_1$. In polar coordinates, with radial coordinate r and azimuthal angle φ , this transformation is given by

$$r \to r' = \frac{R_2 - R_1}{R_2} r + R_1,$$
 (1)

for $0 \le r \le R_2$ and r' = r otherwise. The angle is not transformed. The resulting anisotropic tensors of electric permittivity and magnetic permeability starting from vacuum/air have been given [5] and shall not be repeated here.

As can be seen from Fig. 1(a), light avoids a region of width $2R_1$ in which the metal contact can be positioned. By construction, such a cloak appears as homogeneous vacuum/air. This means that one would get the same reflections at the interface between cloak and PV cell as between vacuum/air and the PV cell. If one wanted to eliminate these reflections, an additional antireflection coating or more advanced designs would be required.

A major challenge of this approach lies in the large material contrast and the large anisotropies required. For dielectrics, anisotropies are inherently connected with birefringence, which is highly undesirable here because the aim is to bring all polarizations of light onto the PV cell active area. This means that practical designs must be based on locally isotropic dielectrics. Furthermore, they must be off-resonant to support broadband low-loss operation. As considered by Leonhardt [6], two-dimensional conformal mappings do, in fact, always lead to graded-index structures with locally isotropic refractive indices. In a conformal mapping, the x and γ coordinates are interpreted as the real and imaginary parts of a complex quantity u = x + iy, and likewise u' = x' + iy'. For a conformal map according to $u \rightarrow u' = f(u)$, the equivalent graded refractive index distribution results from [6]. Any conformal map is infinitely extended in the complex plane. Unfortunately, this means that the resulting invisibility structure

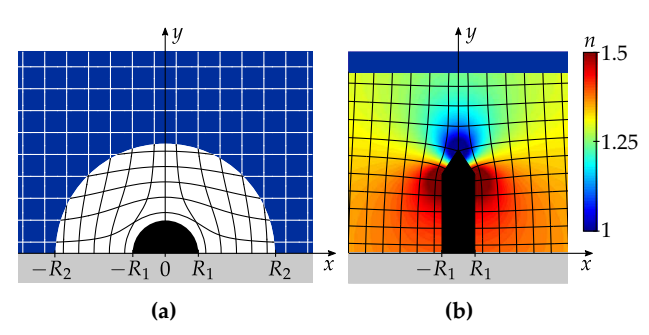


Fig. 1. Coordinate transformations enabling invisible contacts on solar cells. The elongated metal contact to be made invisible can be arbitrarily shaped within the black region. (a) Transformation of a point to a circle with diameter $2R_1$ leading to anisotropic magnetodielectric material distributions (white region). (b) Schwarz–Christoffel conformal map leading to an isotropic graded-index structure with $n(x, y) \in [0, \infty[$ (color-coded). For the realization, we truncate the refractive index to the interval [1.0, 1.5] and fill the forbidden region (black) with full material (n = 1.5).

on top of a metal contact is infinitely large, too. However, it can be truncated approximately, thereby leading to a finite-size structure.

Different conformal maps have been discussed [6–8]. Here, we divide the space on top of the PV cell into a left and a right half. A Schwarz–Christoffel transformation [9] conformally maps each half-space onto a polygon, as illustrated in Fig. 1(b). The charm of this particular transformation is that the expression obtained for the refractive index distribution, $n(u) = |\mathrm{d}f/\mathrm{d}u|^{-1}$, is analytic (see Supplement 1). Nevertheless, the index distribution contains singularities that need to be eliminated for any practical design. Therefore, we truncate the refractive-index profile to the interval from 1.0 to 1.5, which allows for the use of ordinary constituent materials such as polymers or silica glass.

By design, the resulting untruncated structure works perfectly under normal incidence of light, both in wave optics and in ray optics. Here, we focus on ray optics though, because the envisioned metal contacts are many tens or hundreds of wavelengths in size. Consistently, plasmonic effects at the metallic contact fingers are neglected. With truncation with respect to spatial extent and refractive index, the performance is still excellent under normal incidence of light (see Supplement 1). Light impinging under normal incidence and propagating according to the conformal map accumulates the same phase or time-of-flight as though contact and cloak were not there. As pointed out above, this aspect is necessary in the context of true invisibility cloaking but not important for efficient energy conversion.

We also consider an even simpler approach, which ignores the phase (or time of flight) of light altogether. This approach is illustrated in Fig. 2: the goal is to avoid light rays hitting the contact centered around x=0 in the region $|x| \leq R_1$ and spread the light evenly within the remaining region $|x| \in [R_1, R_2]$. In analogy to Pendry's cloaking transformation of a point to a circle [5] just discussed, we can accomplish this goal by the one-dimensional linear coordinate transformation

$$x' = \frac{R_2 - R_1}{R_2} x + R_1,$$
 (2)

for $x \ge 0$, which we shall assume from now on. The left half is the mirror image. The region with $|x| > R_2$ remains untransformed, i.e., x' = x. Next, we map every light ray arriving under normal incidence at coordinate x at height y > 0 onto the transformed coordinate x'(x) on the wafer surface at y = 0.

For a homogeneous dielectric material with constant refractive index n in between, the rays are straight lines. Thus, the angle $\alpha = \alpha(x)$ with respect to the surface normal is given by

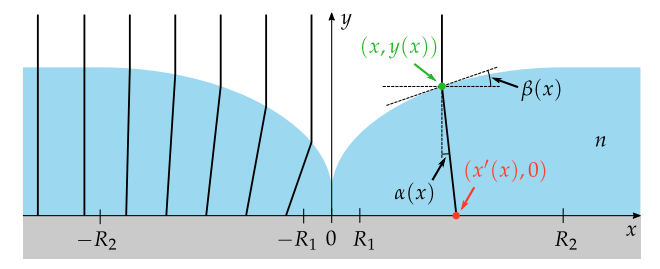


Fig. 2. One-dimensional linear coordinate transformation $x \to x'$ of a point to a finite interval with width $2R_1$ leading to an angle distribution $\alpha(x)$. This distribution can be realized by a freeform surface y(x) of a dielectric with constant refractive index, n, on top of the solar cell. The local surface inclination angle is denoted by $\beta(x)$.

Letter Vol. 2, No. 10 / October 2015 / Optica 852

 $\tan(\alpha) = (x'-x)/y$. The change in angle at the interface can be achieved in different ways. For example, flat optics by designer metasurfaces could be used [10]. It is challenging to obtain broadband and low-loss operation, though. A second way is to use refraction and incline the air–dielectric interface by an angle β with respect to the horizontal (x axis) as a function of x in small intervals, leading to a graded sawtooth shape. We follow a third approach, which uses a smooth freeform surface y = y(x). The geometry and Snell's law lead to an implicit equation for the surface tilt angle $\beta = \beta(x)$ with respect to the horizontal. Integration of $dy/dx = \tan(\beta)$ leads to the height profile y(x) (see Supplement 1 for details). The resulting nonlinear differential equation for $\beta(x)$ can be solved numerically without further approximations; alternatively, it can be solved analytically within the limit of small angles (see Supplement 1).

Corresponding results for the numerical solution are shown in Fig. 2. Obviously, the structure can again be seen as just some lens. Indeed, for $R_1 = R_2$, one gets a lens that focuses light rays to a common point on the PV cell surface. For the more relevant choice of $R_1 < R_2$, the lens rather avoids sending light onto the metal contact area and distributes it evenly onto the regions in between adjacent contacts. By design, the structure operates perfectly for normal incidence of light rays—for different possible choices of R_2 and y(0). We thus exploit these two parameters to further optimize the performance for oblique incidence of light. Notably, such freeform surfaces can potentially be massmanufactured in a cost-effective way by making a master and using it for imprinting, e.g., of inexpensive polymers.

To prove the principle, we have fabricated the designed graded-index structures as well as the dielectric freeform surfaces. Examples of corresponding electron micrographs as well as optical measurements are depicted in Fig. 3.

All structures are made using three-dimensional direct laser writing (DLW, see Supplement 1) of polymers ($n \approx 1.5$) directly onto a silicon wafer on which 20 µm wide and 60 nm thick gold strips (modeling reflective metallic contact fingers) have been prefabricated by standard electron-beam lithography. The gradedindex profile is mimicked by a woodpile photonic crystal used in the long-wavelength limit [11,12]. The local woodpile polymer volume filling fraction is adjusted to give the desired refractiveindex profile [11,12]. Due to resolution restrictions in rapid galvoscanning DLW, the woodpile rod spacing is limited to a = 800 nm. As a result, the operation wavelength cannot be smaller than 1.5 µm [11]. In principle our concept can also be transferred to the visible, although smaller rod spacings are needed. To allow for direct comparison, we use the same characterization setup and the same infrared wavelength for the freeform surfaces (although they do not underlie the same restriction).

A semiconductor diode laser emitting at $1.5~\mu m$ wavelength is coupled into a single-mode optical fiber. Its output is imaged onto the sample and the photocurrent, detected by a large-area germanium photodiode butt-coupled to the silicon wafer, is recorded as a function of the spot's x coordinate. If the spot hits the contact without any polymer structure on top, the photocurrent drops to values near zero (see Fig. 3). In sharp contrast, with cloak, the photocurrent on the contact is nearly as large as that without any structure on the silicon wafer. On the sides of the contact, the photocurrent also slightly rises because the polymer slab effectively acts like an antireflection coating on the air–silicon surface. This aspect is beneficial but represents an indirect side aspect.

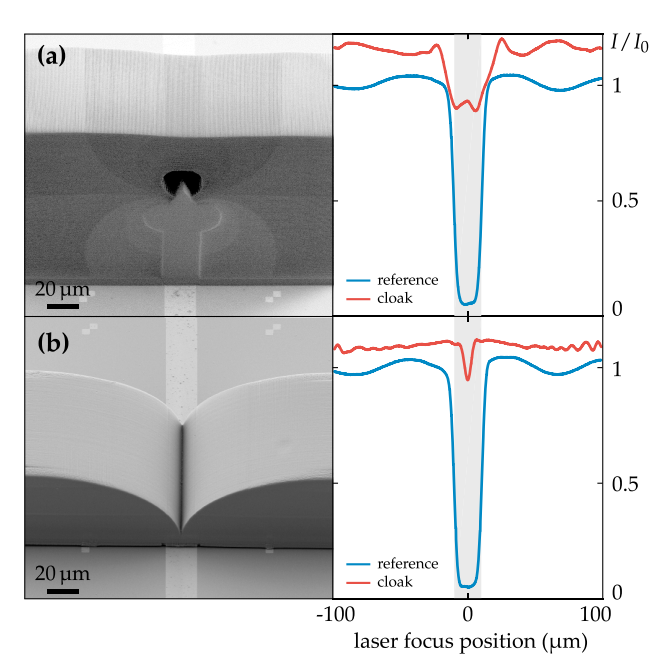


Fig. 3. Electron micrographs of fabricated polymer structures (left) and measured detector signals with metal contact, with (red curve) and without (blue curve) invisibility structure on top (right). The detector signal, I, is normalized to the value far away from the contact, I_0 . (a) Graded-index structure following Fig. 1(b). (b) Freeform surface following Fig. 2, with y(0) = 12 μm, $R_1 = 12$ μm, and $R_2 = 100$ μm.

Importantly, the two approaches, the graded-index structure and the freeform surface, deliver comparable performance under normal incidence of light, thus providing an experimental proof of principle.

Next, we discuss theoretically the behavior of the different invisibility structures for oblique incidence of light. For these calculations, we have implemented a home-built ray-tracing software program including (multiple) angle-dependent Fresnel reflections at all involved interfaces averaged over the polarization of light. We also average over different incident positions of the light rays. However, to separate the direct effects of guiding the light around the contact and the indirect effects due to changes in effective reflectivity, we neglect any partial reflection in the calculations shown in Fig. 4, corresponding to fictitious ideal antireflection coatings at all interfaces. In this fashion, the discussion becomes universal and independent from device and material specifics.

As an example, we consider a periodic arrangement of contact fingers with width $w = R_1/0.6$ and with 10% areal filling fraction on the solar cell in Fig. 4(a). The two free parameters for the freeform structure, i.e., $y(0)/R_1 = 1$ and $R_2/w = 5$, have been chosen according to an optimization regarding angle dependence (see Supplement 1). Figure 4(a) shows that all invisibility structures perform well for incidence angles below 20°, and that the freeform surface fully recovers the 10% shadowing effect even for higher incidence angles. This means that, for example, an initial overall solar cell efficiency of 20% would increase to 22%. When additionally accounting for partial reflections (see Supplement 1) the improvement is even larger, but the precise value depends on the substrate refractive index and on what structure one references the performance to. Interestingly, replacing the full material (n = 1.5) in the forbidden region of the graded-index structure by air drastically improves the performance of the graded-index **Letter** Vol. 2, No. 10 / October 2015 / Optica 853

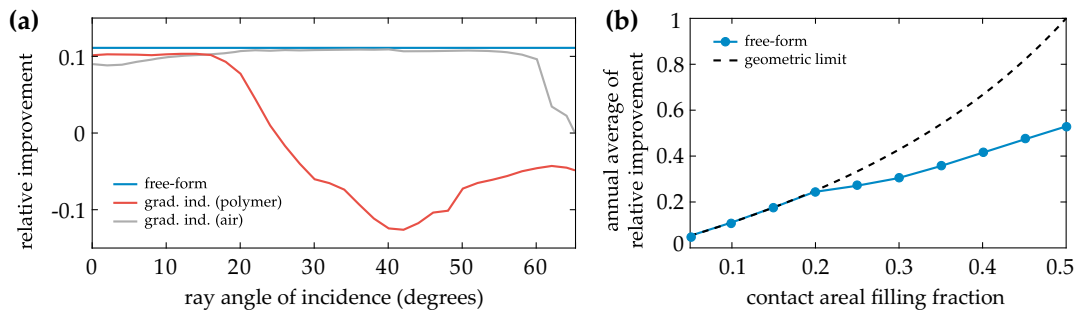


Fig. 4. (a) Calculated relative improvement $\zeta = (N - N_{\rm ref})/N_{\rm ref}$ due to the invisibility structure on top of the periodic arrangement of metal contacts with width $w = R_1/0.6$ versus ray angle of incidence with respect to the surface normal, neglecting partial reflections. Here, N is the number of light rays hitting the silicon surface with invisibility structure and $N_{\rm ref}$ is that without this structure. As an example, we assume 10% area coverage of the metal contacts, leading to a maximum possible relative improvement $\zeta_{\rm max} = 0.1/0.9 \approx 11\%$. Graded-index structure as in Fig. 1(b) with polymer core (red curve), air core (gray curve), and transformed freeform surface (blue curve) as in Fig. 2 (with $R_2/w = 5$, $y(0)/R_1 = 1$, and n = 1.5). (b) Calculated average annual relative improvement due to the freeform surface, $\langle \zeta \rangle$, versus areal fraction covered by the contact (blue curve). The dashed curve represents the maximum possible relative improvement $\zeta_{\rm max}$.

structure for more oblique angles. This can be explained by total internal reflection of rays that hit the air core, hindering them from entering the forbidden region.

Figure 4(b) presents the average of the relative improvement over the calendar year for the freeform surface with varying contact areal filling fraction. The calculation is carried out for global radiation under Karlsruhe conditions (see Supplement 1). For filling fractions up to 20%, a complete elimination of the contact shadowing effect can be observed. Thus, with a freeform invisibility structure, one could reduce the Ohmic losses in the contact grid by drastically increasing its density without adding optical losses.

In conclusion, we have designed different practical invisible contacts on solar cells by coordinate transformations. We have shown that transformed freeform polymer surfaces provide complete remedy of the shadowing problem. Potentially, these structures can even be mass-manufactured. It is also easier for these structures to obtain operation throughout the entire visible spectrum. The concept is also applicable to encapsulated solar cells (see Supplement 1) and can be transferred to other optoelectronic devices where efficient coupling to light at minimum electric losses is crucial, e.g., light-emitting diodes or optical detectors.

Funding. Deutsche Forschungsgemeinschaft; German Academic Exchange Service (Deutscher Akademischer Auslandsdienst); Karlsruhe School of Optics & Photonics;

Open Access Publishing Fund of Karlsruhe Institute of Technology.

Acknowledgment. We thank Michael Thiel (Nanoscribe GmbH) for help with the sample fabrication.

See Supplement 1 for supporting content.

REFERENCES

- 1. H. Booth, J. Laser Micro/Nanoeng. 5, 183 (2010).
- 2. A. Meulenberg, J. Energy 1, 151 (1977).
- C. Vogeli and P. Nath, "Photovoltaic device with decreased gridline shading and method for its manufacture," U.S. patent 5, 110, 370 (May 5, 1992).
- J. Schneider, M. Turek, M. Dyrba, I. Baumann, B. Koll, and T. Booz, Prog. Photovoltaics 22, 830 (2014).
- 5. J. B. Pendry, D. Schurig, and D. R. Smith, Science 312, 1780 (2006).
- 6. U. Leonhardt, Science 312, 1777 (2006).
- R. Schmied, J. C. Halimeh, and M. Wegener, Opt. Express 18, 24361 (2010).
- 8. J. C. Halimeh and M. Wegener, Opt. Express 21, 9457 (2013).
- T. A. Driscoll and L. N. Trefethen, Schwarz-Christoffel Mapping (Cambridge University, 2002).
- 10. N. Yu and F. Capasso, Nat. Mater. 13, 139 (2014).
- T. Ergin, N. Stenger, P. Brenner, J. B. Pendry, and M. Wegener, Science 328, 337 (2010).
- 12. J. Fischer, T. Ergin, and M. Wegener, Opt. Lett. 36, 2059 (2011).